

Shape memory effect in cross-linked polyethylene matrix composites: the effect of
the type of reinforcing fiber

Tatár B., Mészáros L.

Accepted for publication in Polymer Bulletin

Published in 2024

DOI: [10.1007/s00289-023-05003-0](https://doi.org/10.1007/s00289-023-05003-0)



Shape memory effect in cross-linked polyethylene matrix composites: the effect of the type of reinforcing fiber

Balázs Tatár¹ · László Mészáros^{1,2}

Received: 11 May 2023 / Revised: 7 September 2023 / Accepted: 8 September 2023 /
Published online: 23 September 2023
© The Author(s) 2023

Abstract

The recovery stress of shape-memory polymers is often low; therefore their field of application is limited. In this study, we compared the effects of different fiber reinforcements on the shape memory characteristics of cross-linked polyethylene (X-PE) matrix. We used fiber reinforcement to increase the recovery stress of the shape memory polymer and compared the results of different fiber reinforcements to find the ones that confer the best shape memory properties. We investigated glass, carbon, Kevlar[®], and Dyneema[®] fibers to find the fibers that increase the recovery stress of the composites most. The deformed shape was created by three-point bending, and then heat-activated shape recovery was examined. All reinforcements increased the recovery stress and decreased the shape fixity ratio and the shape recovery ratio. The samples had similar characteristics, except for the low recovery stress Kevlar[®] fibers and the low recovery ratio of the composite reinforced with glass fibers. With the polyethylene Dyneema[®] fibers, the composite was self-reinforced and did very well by all metrics. They increased the maximum recovery stress from 0.3 to 2.4 MPa, through having excellent adhesion to the matrix and high strength in their own right. Our research proved that self-reinforced composites could measure up to conventional composites in shape memory applications. Aside from the Dyneema[®] fibers carbon fibers work best in the X-PE matrix, and should be the preferred conventional reinforcement materials.

Keywords Shape memory polymers · Recovery stress · Cross-linked polyethylene · Ionizing radiation · Compression molding · Thermoplastic composites

✉ László Mészáros
meszaros@pt.bme.hu

¹ Department of Polymer Engineering, Faculty of Mechanical Engineering, Budapest University of Technology and Economics, Műegyetem rkp. 3., Budapest 1111, Hungary

² HUN-REN-BME Research Group for Composite Science and Technology, Műegyetem rkp. 3., Budapest 1111, Hungary

Introduction

Shape memory materials are intelligent materials capable of recovering their original shape from a programmed shape in response to a non-mechanical stimulus [1]. They include both shape-memory alloys and shape-memory polymers (SMP). They have now found applications in many fields, such as the space industry, biomedicine, joining, and packaging [2, 3].

SMP-s have quite a few advantages compared to metallic alloys; they have a lower density, and they are more economical to produce and have higher achievable strains. On the other hand, they have much lower recovery stresses (σ_{rec}), which limits their application in fields where recovery under load is required [4].

For the shape memory effect, the polymer needs to have a dual structure. It needs switches and netpoints in the polymer, which are bonds or phases. Shape memory can be triggered by many stimuli, but the most common stimulus is heat. In this case, for a shape memory cycle, first, the SMP is heated above its transition temperature, where the switches release, for example, with the crystalline phase melting. The material then can be deformed into its programmed shape, only being held together by the netpoints, for example, by cross-links between molecules. Then in shape, the SMP needs to be cooled down so that the switches close; when the load is released, the netpoints store some of the internal energy resulting from the deformation. When the switches are released next, without external loads, this energy can bring the SMP back to its original shape [5].

One of the most effective ways of improving σ_{rec} for SMPs is using fiber reinforcement. While fiber reinforcement improves the recovery stress, it can adversely affect the precision of the recovery, characterized by the shape fixity ratio (R_f) and the shape recovery ratio (R_r), as defined in Eqs. 1 and 2.

$$R_f = \frac{\varepsilon_u}{\varepsilon_m}, \quad (1)$$

$$R_r = \frac{\varepsilon_m - \varepsilon_p}{\varepsilon_m}, \quad (2)$$

where ε_m is the maximum strain applied to the specimen, ε_u is the strain after unloading at low temperature, and ε_p is the persisting strain after recovery [6].

Researchers have experimented with many types of SMPs and fiber reinforcements so far to create more efficient SMP composites. Glass fibers, widely used in the composite industry, have seen application in shape memory epoxy resins and shape memory polyurethanes as well [7, 8]. Fejős et al. [9] reinforced epoxy resin with woven glass fiber fabric to an approximate 38 vol% fiber content. They found that the reinforcement had greatly increased the flexural modulus and recovery stress. They found no decrease in the recovery ratio but a substantial decrease in the fixity ratio. Rahman et al. [10] added chopped glass fibers up to 30 vol% to shape memory polyurethane. Increasing glass fiber content increased material strength considerably but had little effect on shape recovery. The shape fixity ratio decreased with increasing fiber content, which the researchers explained with the decreasing

volume fraction that takes part in the glass transition, which is the driving force for the phenomenon. Liu et al. [11] made composites for dental applications with up to 40 wt% short glass fibers and a polyurethane matrix. Glass fibers had a negative effect on shape recovery, reducing it from 85 to 73%. The authors explained this with the limiting effect of glass fibers on molecular mobility. The 40 wt% composite had a recovery force increased by 96% compared to the reference. Glass fibers are widely used, sturdy fibers that can very effectively increase the recovery stress, but usually have a negative effect on the precision of recovery.

Carbon fiber is also an often-used reinforcing material for shape memory polymers [12–14]. Li et al. [15] added 37 wt% carbon fiber into a shape-memory epoxy resin and for 5% deformation experiments, obtained an increase from 16 to 47 MPa in recovery stress. In free recovery experiments, there was a slight decrease in the fixation ability of the polymer but no quantifiable decrease in its recovery capability. Carbon fibers have a lower density and seem to have better effects on shape memory, but are also more expensive than glass fibers.

Kevlar® fibers seldom appear as reinforcement in shape memory composites. Jing et al. [16] compared the performance of Kevlar® fibers with that of carbon fibers and found that increasing amounts of both fibers affected fixity and recovery performance adversely, with Kevlar® performing better in fixity and carbon in recovery. Kevlar® fibers are rarely investigated as reinforcement in shape memory composites. Their great flexibility could adversely affect the recovery stress but improve the precision of recovery.

Emanuel et al. [17] compared the effect of basalt fiber reinforcement to carbon and glass fiber reinforcement in epoxy resins on shape memory properties. They observed that carbon fiber composites had the lowest R_f but the fastest recovery. Glass and basalt fiber composites recovered at about the same rate. In tensile tests, the carbon fibers performed best, while basalt fibers produced slightly higher modulus and strength than glass fibers.

Maksimkin et al. [18] investigated the shape memory effect of ultra-high molecular weight polyethylene (UHMWPE) fibers. Although PE does not have chemical cross-links, the high molecular weight of the polymer means that the amorphous chain entanglements can fix the permanent shape while the crystalline domains keep the temporary shape. They compared these results to UHMWPE in bulk state, which also exhibited shape memory for the same reasons, and found that the fibers had considerably higher recovery stress compared to the bulk samples. The shape memory properties of UHMWPE can be improved by cross-linking [19], a process through which thermoplastic polyethylene (PE) obtains shape memory properties as well [20].

There are two popular methods for the cross-linking of polyethylene: using ionizing radiation or chemical cross-linking agents. Both serve to separate a hydrogen atom from the polymer backbone, creating a reactive free radical that can combine with a free radical on another chain, so a cross-link is formed. Such linkage can also happen between the polymer and a filler embedded in it, enhancing the strength of the connection between them. Out of the two, the chemical method can only take place in the molten state of the polymer (as the cross-linking agent needs to be dispersed), while radiation cross-linking can happen in the solid state. In the case of

semi-crystalline polymers, irradiation yields cross-links in the amorphous phase and leads to a cross-linked and also semi-crystalline polymer [20]. In this structure, from the viewpoint of shape memory, the cross-links serve as the net points and the crystalline phase as the switches.

Cross-linked polyethylene (X-PE) made from low-density polyethylene (LDPE) can then be used as a matrix and reinforced with the UHMWPE fibers mentioned above to form a self-reinforced composite [21]. The influence of self-reinforcement on shape memory properties has not yet been investigated. The high strength of UHMWPE fibers is similar to that of other fibers, but their high elasticity may limit their use. On the other hand, since they can take part in the shape memory effect, they could prove very effective.

There is also not much literature on the shape memory properties of conventional X-PE composites. Wang et al. [22, 23] conducted experiments on cross-linked poly(styrene-*b*-butadiene-*b*-styrene) triblock copolymer/X-PE blends reinforced by short glass and carbon fibers. They found that glass fiber reinforcement slowed recovery but in repeated recovery tests, it increased R_r . With carbon fibers, they found a slower recovery, and an increase in R_r and a decrease in R_t with increasing fiber content.

In this study we compare the most often used and some novel fiber reinforcement materials with regard to their effect on shape memory. We chose cross-linked polyethylene irradiated by gamma rays as the matrix, in part for the potential compatibilizing effect of the irradiation and in part to give Dyneema® fibers a self-reinforcing potential, which has seldom been investigated in the literature before. We also used carbon and glass fibers because they are the most commonly used fibers in composites, and their high stiffness compared to polymer fibers is expected to increase recovery stress significantly. We added Kevlar® fibers to the experiment to have another polymeric fiber with high elasticity besides the Dyneema® fibers. Kevlar® fibers also have high strength and modulus. We investigated the composites manufactured from the fibers for constrained and free recovery to get a comprehensive picture of their shape memory characteristics.

Materials and methods

Materials used

To make composites, we used LDPE (later irradiated to make X-PE) as a matrix. In all cases, the matrix was the DOW LDPE PG 7008 (Dow Chemical Company, USA) resin. According to its datasheet, it has a density of 0.918 g/cm³, a melt flow index (MFI) of 7.7 g/10 min (190 °C, 2.16 kg), a tensile modulus of 160 MPa and a tensile strength of 8 MPa. Different fibers were used as reinforcement: ZOLTEK PX35 carbon fiber (Zoltek Zrt., Hungary), Advantex® SE 1200 E-glass fiber (Owens Corning Ltd., USA), Kevlar® 29 aramid fiber (DuPont de Nemours Inc., USA), and Dyneema® SK76 polyethylene fibers (Koninklijke DSM N. V., Netherlands). Table 1 contains the most important characteristics of these fibers.

Table 1 Basic properties of the fibers and composites

Fiber type	Carbon	Glass	Kevlar	Dyneema
Fiber diameter [μm]	~ 7.2	13–23	~ 12	12–21
Density [g/cm^3]	1.81	2.62	1.44	0.975
Modulus [GPa]	242	81	70.5	130
Tensile strength [MPa]	4137	2700	3600	3600
Thickness of the composite [mm]	2.10 ± 0.01	2.03 ± 0.02	2.12 ± 0.02	2.50 ± 0.04

Production of shape memory materials

We used a Tech-Line Platen Press 200E hot press (Dr. Collin GmbH, Munich, Germany) to press the granules into 0.5 mm thick 160×160 mm sheets at 120°C with a pressure of 7 bar. Then 5-layer composites were made with these sheets, with 2 unidirectional fiber layers, with a total of 30 w/w% fiber content, because the densities of the fibers were different, this resulted in slightly different thicknesses for different reinforcing fibers. Individual rovings were taken from fabrics, and in the case of the Dyneema fiber, wound onto the pressing frame from a spool. We then hot-pressed the stacked components again at 120°C to produce the composites. One half of the composite sheets prepared this way were then exposed to gamma irradiation. A panoramic SLL-01 ^{60}Co radiation source was used at the Institute of Isotopes Ltd. (Budapest, Hungary), at a rate of 10 kGy/h for an absorbed dose of 150 kGy, which we chose for cross-linking in the preliminary experiments.

Characterization methods

Soxhlet extraction

The Soxhlet extractions were performed on an R 256 S extractor (BEHR Labor Technik GmbH, Germany); the extractions lasted for 24 h and used a boiling mixture of xylene isomers as a solvent. Irradiated and non-irradiated unreinforced polyethylene samples were investigated, and we did all the experiments three times. We placed ~ 1 g samples in cellulose sample holder capsules and dried them for 3 h at 60°C in a drying oven before weighing them and placing them in a random order in the extractor. We then calculated the gel fraction by dividing the initial mass by the leftover mass after extraction.

Scanning electron microscopy (SEM)

We produced scanning electron microscopic (SEM) images of the cross-section of the samples. The cross-sections were produced by cutting at ambient temperature. The surfaces were sputtered with a thin layer of gold before the examination. The

scanning electron microscope was a JEOL JSM 6380LA SEM (Jeol Ltd., Japan). Secondary electron imaging and an acceleration voltage of 10 kV were used.

Bending tests

Bending tests were conducted on 50 mm long and 10 mm wide specimens, with the thickness depending on the type of reinforcement (Table 1), because of differing fiber densities. We tested five specimens of each type on a Zwick Z005 MT universal testing machine (Zwick GmbH., Germany). Testing speed was 4 mm/min, and the conventional deflection was 4 mm in accordance with EN ISO 178:2019. We calculated the bending modulus as the slope of the tangent at the initial straight part of the bending curve.

Free recovery experiments

We studied the shape memory properties of the samples in two experiments: free recovery and constrained recovery. The free recovery experiments were conducted on a Zwick Z250 universal testing machine (Zwick GmbH., Germany) equipped with a heating chamber. We placed the 50 mm long and 10 mm wide specimens in a 3-point bending head with a 40 mm gauge length. Then they were heated in the heating chamber to 100 °C, which is within their melting temperature range, and kept at this temperature for 5 min. They were then bent from a 180° (flat) shape to a ~100° bent shape by displacing the middle of the specimen by 13 mm. The bent shape was fixed by removing the bending head from the heating chamber and leaving it at room temperature for 5 min (Fig. 1). The programmed shape was then measured by a digital protractor. The shape was recovered by heating the specimen at 100 °C for 5 min in the bending head without load. Then we measured the recovered shape, the

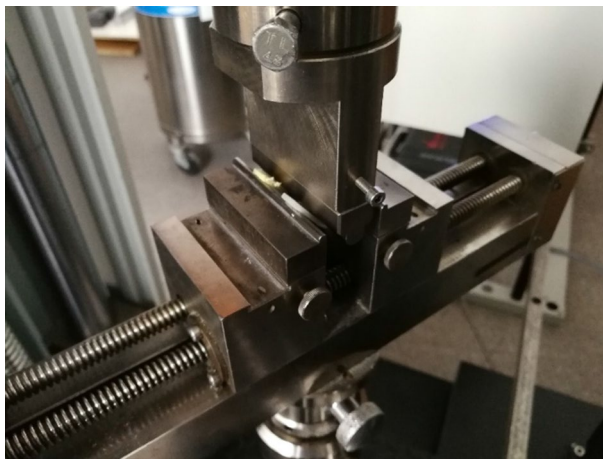


Fig. 1 The measurement setup for the free recovery experiments

bending angle in the middle, with the protractor and calculated the flexural strain (ε) from the angle (α) using Eq. (3):

$$\varepsilon = \frac{3 \cdot \cos(\alpha/2) \cdot h}{L} \quad (3)$$

where L is the support distance and h is the thickness of the composite and α is the angle at which the specimen is bent.

Constrained recovery experiments

The constrained recovery experiments were conducted in a Q800 dynamic mechanical analyzer (DMA) (TA Instruments Inc., USA). The samples were 10×40 mm with varying thicknesses (Table 1). The samples were tested with a gauge length of 20 mm with a 3-point bending clamp. During testing, the samples were heated to 100 °C. They were then bent to a 2 mm displacement in 1 min, and cooled to 30 °C, while the displacement was kept, and then external force was released. Subsequently, a 0.03% constant flexural strain was applied on the samples to ensure firm contact with the clamp head and no change in displacement. Under these conditions, they were reheated to 100 °C at a rate of 5 °C/min while the stress generated was recorded and we took the maximum of these curves to characterize each sample.

Results and discussion

Soxhlet extraction

We used Soxhlet extraction to quantify the extent of cross-linking in the samples through the gel fraction of the samples. In the extractions, all of the unirradiated samples dissolved completely (yielding a gel fraction of 0%), while all irradiated samples produced a leftover mass, indicating that all of the gel fraction resulted from cross-linking via irradiation. The average gel fraction of the irradiated samples was 57.6%, which is more than Rezanejad and Kokabi found [24] for peroxide-initiated cross-linking, which was 48% for unfilled samples. They achieved a great shape memory effect with this material. Because of this, we judged the gel fraction (and cross-linking) high enough for the shape memory effect to manifest due to the cross-linked structure.

SEM microscopy

We used SEM images to characterize the structure of the composites (Fig. 2). The images show that most of the fiber reinforcement remained in two separate rovings and did not get completely mixed up with the matrix, just as we expected, due to the high viscosity of the matrix (at the temperature required to avoid the melting of the Dyneema® fibers). All fibers remained intact through the processing and kept their shape. It is also clear that the matrix did not completely wet the fiber rovings, but

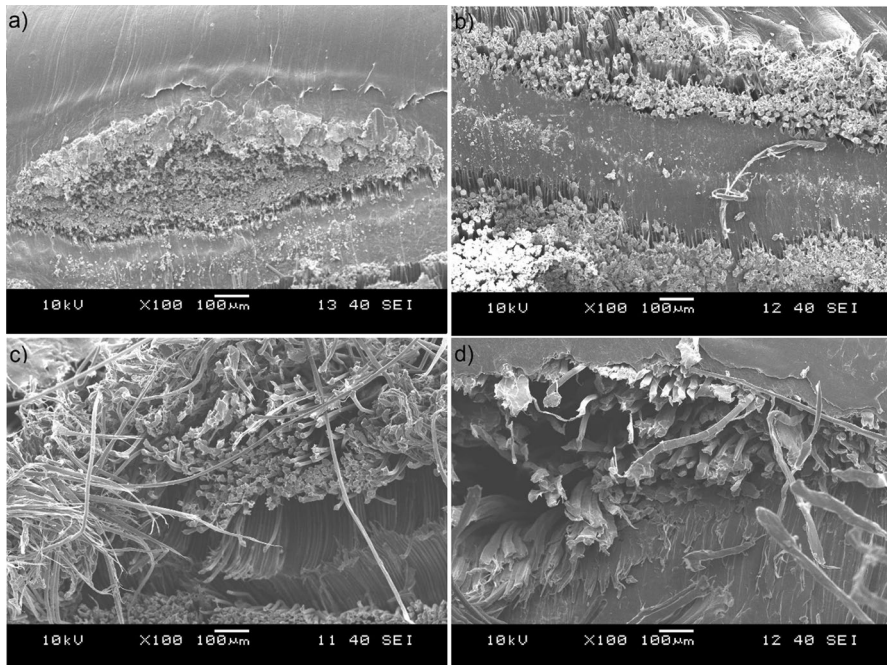


Fig. 2 The SEM images of the cut surfaces of the composites reinforced with: **a** carbon fibers, **b** glass fibers, **c** Kevlar® fibers, and **d** Dyneema® fibers

the fibers stuck well to the matrix where they had contact. From the SEM images, it can also be concluded that the fibre-matrix contact was the best when Dyneema® was used. It can also be seen that non-saturated roving portions remained in some composites, especially in the glass fibre-reinforced case. The presence of voids was expected, however, in the case of long fibre reinforcement the mechanical reinforcement is still significant. In the case of the Kevlar® and Dyneema® fiber-reinforced samples, the fibers pulled out more because of the difficulty of cutting these fibers. The imperfections in impregnation, however, did not impair bending resistance so much. Also, we kept bending displacements relatively small to avoid any possible issues.

Bending tests

Bending tests were conducted to quantify the relevant mechanical properties of each sample. During the bending tests, different samples exhibited different types of behavior. The carbon fiber and Dyneema® fiber-reinforced samples showed a decrease in stress before reaching the convention deflection while not breaking completely (Fig. 3), similar to the behavior reported by Li et al. [15] and Deng and Shalaby [25]. On the other hand, the glass and Kevlar® fiber-reinforced samples showed a sharp change in their resistance at one point but stress continued to increase with

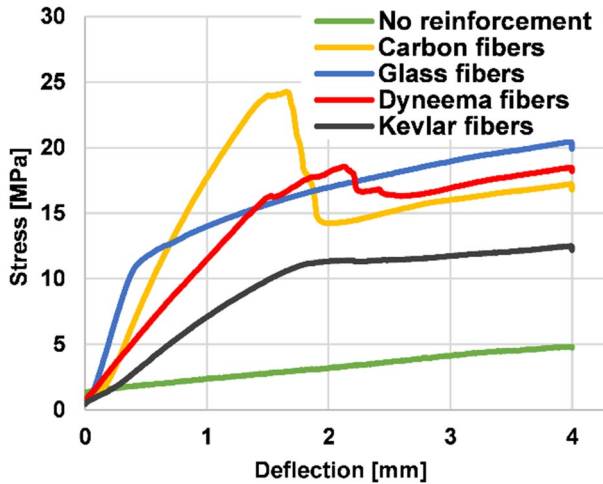


Fig. 3 Representative bending curves for the irradiated samples with different fiber reinforcements

deflection. The first response of the Dyneema[®] and carbon fiber-reinforced samples can be attributed to the effects of fiber breakage and slipping, while the second response of the glass and Kevlar[®] fiber-reinforced samples to partial fiber–matrix debonding. These findings are in accordance with the visual observations during testing as well. The unreinforced reference produced an almost linear bending curve, which was at all points below that of the reinforced samples. Thus, all fibers reinforced the matrix (Fig. 4).

Glass fiber reinforcement produced the highest modulus, while carbon fiber reinforcement produced the highest strength (Fig. 5). While the Dyneema[®]

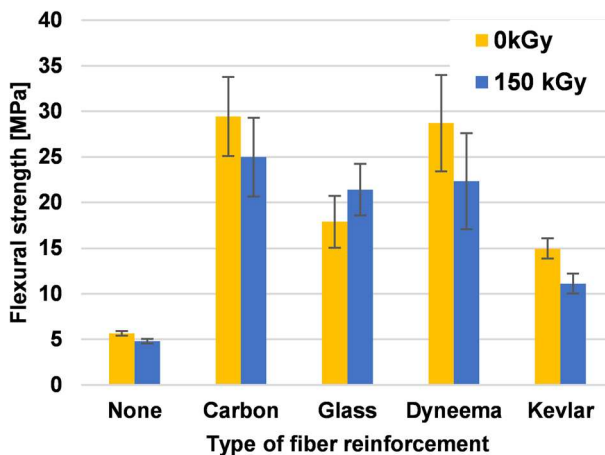


Fig. 4 Flexural strength or stress at convention deflection of samples

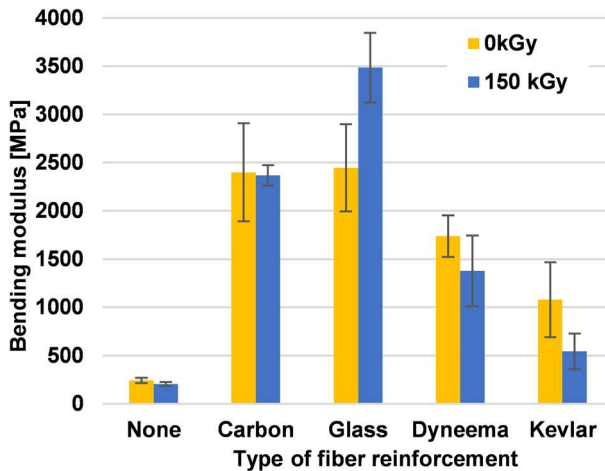


Fig. 5 The bending modulus of samples

fiber-reinforced sample had a far lower modulus compared to the glass fiber-reinforced and carbon fiber-reinforced samples, it did not fall behind in strength. Irradiation decreased the strength and modulus of the specimens in all cases except for the glass fiber-reinforced specimen, which is probably due to the compatibilizing effect of the irradiation. This sample had a modulus close to 3500 MPa, which is high for a composite like this.

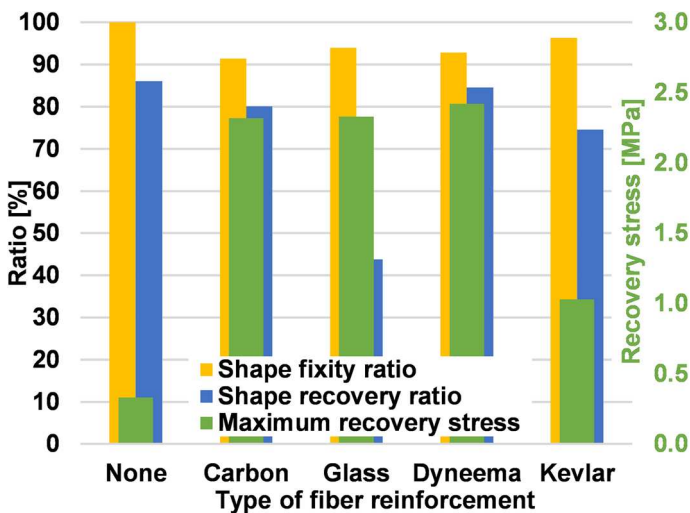


Fig. 6 Shape memory characteristics of the samples

Free recovery experiments

In the free recovery experiments, the specimens were allowed to complete their shape recovery. All of the specimens investigated demonstrated shape memory behavior (Fig. 6). The cross-links allowed the material structure to store the internal stresses resulting from the programming, and when crystalline melting allowed it, that stress was released, and returned the specimen to its original shape. The shape fixity ratio (R_f) for the unreinforced sample was 100% and decreased by 5–10% for all types of reinforcement. This observation is slightly in contrast with Wang et al. [23] who found a slight increase in R_f with increasing carbon fiber content, in either case fiber reinforcement had little effect R_f . All of the composites yielded very similar results within 5% of each other. This discrepancy is probably due to the fact that some fiber slippage occurred in the reinforced samples, leading to some permanent deformation. The shape recovery ratio (R_r) of different reinforcement types differed more. Again, the unreinforced sample performed best, with the Dyneema® and carbon fiber-reinforced samples close behind. The findings of Wang et al. [22, 23, 26] confirm this. They found only a small decrease in R_r in the case of 12 wt% carbon reinforcement, but a large one in case of only 2.5 wt% glass reinforcement. The largest decrease in our study was in the case of the glass reinforcement, where it plummeted to 44%, likely because of the inflexibility of the glass fibers, which prevented recovery. Kevlar® fiber-reinforced samples were between the two groups. The reduction in R_r probably occurred due to the increased modulus of the samples and because the fibers did not contribute cross-links to the recovery, except in the case of the PE Dyneema® fiber, which is also capable of cross-linking.

Constrained recovery experiments

The main goal of fiber reinforcement in this study was to raise the recovery stress of the specimens. The maximum recovery stress of every composite was several times that of the pure matrix (Fig. 6). The Kevlar® fibers increased recovery stress the least, due to their lower strength, while the composites with glass, carbon, and Dyneema® fibers all had recovery stresses of around 2 MPa, as the reinforcement required a higher stress to deform and thus enabled the material to store more of that stress in the cross-links. Recovery stress correlates well with bending strength but less so with modulus. This indicates a connection between recovery stress and bending strength.

Conclusions

We investigated X-PE composites with different fiber reinforcements (glass, carbon, Kevlar®, and Dyneema® fibers) for shape memory. Each fiber reinforcement greatly increased recovery stress, but reduced shape fixity and shape recovery ratios; however, some fibers did not reduce them considerably. The carbon and Dyneema®

fiber-reinforced samples performed best, with high recovery stresses and shape memory ratios. Recovery stress correlated most with bending strength, as with higher strength, the specimen can store more of the programming load as internal stress for the recovery. Kevlar[®] fiber reinforcement increased recovery stress only to about half of that of the other reinforcements because of its high flexibility. The glass fiber composite, on the other hand, had a much lower recovery ratio because its inflexibility inhibited the composite's recovery. Dyneema[®] fibers are made from polyethylene, therefore the Dyneema[®] fiber-reinforced composite was a self-reinforced composite. Its highest overall performance indicates that this reinforcement is a viable alternative to standard reinforcing fibers.

Acknowledgements Project no. TKP-6-6/PALY-2021 has been implemented with the support provided by the Ministry of Culture and Innovation of Hungary from the National Research, Development and Innovation Fund, financed under the TKP2021-NVA funding scheme. The authors also extend their acknowledgment to the International Atomic Energy Agency (IAEA) for financial support under the umbrella of CRP (Coordinated Research Project). László Mészáros is thankful for the János Bolyai Research Scholarship of the Hungarian Academy of Sciences, and for the ÚNKP-22-5 New National Excellence Program of the Ministry for Innovation and Technology.

Funding Open access funding provided by Budapest University of Technology and Economics.

Declarations

Conflict of interest The authors declare that they have no conflict of interest.

Open Access This article is licensed under a Creative Commons Attribution 4.0 International License, which permits use, sharing, adaptation, distribution and reproduction in any medium or format, as long as you give appropriate credit to the original author(s) and the source, provide a link to the Creative Commons licence, and indicate if changes were made. The images or other third party material in this article are included in the article's Creative Commons licence, unless indicated otherwise in a credit line to the material. If material is not included in the article's Creative Commons licence and your intended use is not permitted by statutory regulation or exceeds the permitted use, you will need to obtain permission directly from the copyright holder. To view a copy of this licence, visit <http://creativecommons.org/licenses/by/4.0/>.

References

1. Bhanushali H, Amrutkar S, Mestry S, Mhaske ST (2022) Shape memory polymer nanocomposite: a review on structure-property relationship. *Polym Bull* 79:3437–3493. <https://doi.org/10.1007/s00289-021-03686-x>
2. Zhang MQ (2022) Shape memory polymer capable of gradual transformation and working. *Express Polym Lett* 16:1011–1011. <https://doi.org/10.3144/expresspolymlett.2022.73>
3. Tatár B, Mészáros L (2023) Shape memory polymers: current state and future prospects. *Express Polym Lett* 17:674–674. <https://doi.org/10.3144/expresspolymlett.2023.49>
4. Behl M, Zotzmann J, Lendlein A (2010) Shape-memory polymers. Springer, Berlin, Heidelberg, Germany
5. Han XJ, Dong ZQ, Fan MM, Liu Y, Li JH, Wang YF, Yuan QJ, Li BJ, Zhang S (2012) pH-induced shape-memory polymers. *Macromol Rapid Comm* 33:1055–1060. <https://doi.org/10.1002/marc.20120153>
6. Jeewantha LHJ, Epaarachchi JA, Forster E, Islam M, Leng J (2022) Early research of shape memory polymer vascular stents. *Express Polym Lett* 16:902–923. <https://doi.org/10.3144/expresspolymlett.2022.66>
7. Wei K, Zhu GM, Tang YS, Li XM, Liu TT, Niu L (2013) An investigation on shape memory behaviours of hydro-epoxy/glass fibre composites. *Compos Part B-Eng* 51:169–174. <https://doi.org/10.1016/j.compositesb.2013.03.036>

8. Asar A, Irfan MS, Khan KA, Zaki W, Umer R (2022) Self-sensing shape memory polymer composites reinforced with functional textiles. *Compos Sci Technol* 221:109219. <https://doi.org/10.1016/j.compscitech.2021.109219>
9. Fejos M, Romhany G, Karger-Kocsis J (2012) Shape memory characteristics of woven glass fibre fabric reinforced epoxy composite in flexure. *J Reinf Plast Comp* 31:1532–1537. <https://doi.org/10.1177/0731684412461541>
10. Rahman AA, Ikeda T, Senba A (2017) Memory effects performance of polyurethane shape memory polymer composites (SMPC) in the variation of fiber volume fractions. *Fiber Polym* 18:979–986. <https://doi.org/10.1007/s12221-017-6687-9>
11. Liu YF, Wu JL, Song SL, Xu LX, Chen J, Peng W (2018) Thermo-mechanical properties of glass fiber reinforced shape memory polyurethane for orthodontic application. *J Mater Sci-Mater M* 29:148. <https://doi.org/10.1007/s10856-018-6157-y>
12. Cheng XY, Chen Y, Dai SC, Bilek MMM, Bao SS, Ye L (2019) Bending shape memory behaviours of carbon fibre reinforced polyurethane-type shape memory polymer composites under relatively small deformation: characterisation and computational simulation. *J Mech Behav Biomed* 100:103372. <https://doi.org/10.1016/j.jmbbm.2019.103372>
13. Leng JS, Lan X, Lv HB, Zhang DW, Liu YJ, Du SY (2007) Investigation of mechanical and conductive properties of shape memory polymer composite (SMPC). In: *Behavior and Mechanics of Multifunctional and Composite Materials 2007*, vol 6526. SPIE. Doi :<https://doi.org/10.1117/12.715510>
14. Guo JM, Wang ZQ, Tong LY, Lv HQ, Liang WY (2015) Shape memory and thermo-mechanical properties of shape memory polymer/carbon fiber composites. *Compos Part A-Appl Sci* 76:162–171. <https://doi.org/10.1016/j.compositesa.2015.05.026>
15. Li FF, Scarpa F, Lan X, Liu LW, Liu YJ, Leng JS (2019) Bending shape recovery of unidirectional carbon fiber reinforced epoxy-based shape memory polymer composites. *Compos Part A-Appl Sci* 116:169–179. <https://doi.org/10.1016/j.compositesa.2018.10.037>
16. Jing XH, Liu YY, Liu YX, Tan HF (2012) Preparation and properties of shape memory epoxy resin composites. *Appl Mech Mater* 214:12–16. <https://doi.org/10.4028/www.scientific.net/AMM.214.12>
17. Emmanuel KDC, Herath HMC, Jeewantha LHJ, Epaarachchi JA, Aravinthan T (2021) Thermo-mechanical and fire performance of DGEBA based shape memory polymer composites for constructions. *Constr Build Mater* 303:124442. <https://doi.org/10.1016/j.conbuildmat.2021.124442>
18. Maksimkin A, Kaloshkin S, Zadorozhnyy M, Tcherdyntsev V (2014) Comparison of shape memory effect in UHMWPE for bulk and fiber state. *J Alloy Compd* 586:S214–217. <https://doi.org/10.1016/j.jallcom.2012.12.014>
19. Chen TH, Li QY, Fu ZW, Sun LW, Guo WH, Wu CF (2018) The shape memory effect of crosslinked ultra-high-molecular-weight polyethylene prepared by silane-induced crosslinking method. *Polym Bull* 75:2181–2196. <https://doi.org/10.1007/s00289-017-2144-6>
20. Peacock AJ (2000) *Handbook of polyethylene: structures, properties, and applications*. Dekker, New York
21. Meszaros L, Tatar B, Toth K, Foldes A, Nagy KS, Jedlovsky-Hajdu A, Toth T, Molnar K (2022) Novel, injection molded all-polyethylene composites for potential biomedical implant applications. *J Mater Res Technol* 17:743–755. <https://doi.org/10.1016/j.jmrt.2022.01.051>
22. Wang YK, Zhu GM, Xie JQ, Men QN, Liu TT, Ren F (2014) An investigation on shape memory behavior of glass fiber/SBS/LDPE composites. *J Polym Res* 21:515. <https://doi.org/10.1007/s10965-014-0515-3>
23. Wang YK, Tian WC, Zhu GM, Xie JQ (2016) Thermomechanical and shape memory properties of SCF/SBS/LLDPE composites. *Chin J Polym Sci* 34:1354–1362. <https://doi.org/10.1007/s10118-016-1838-9>
24. Rezanejad S, Kokabi M (2007) Shape memory and mechanical properties of cross-linked polyethylene/clay nanocomposites. *Eur Polym J* 43:2856–2865. <https://doi.org/10.1016/j.eurpolymj.2007.04.031>
25. Deng M, Shalaby SW (1997) Properties of self-reinforced ultra-high-molecular-weight polyethylene composites. *Biomaterials* 18:645–655. [https://doi.org/10.1016/S0142-9612\(96\)00194-9](https://doi.org/10.1016/S0142-9612(96)00194-9)
26. Wang YK, Zhu GM, Tang YS, Liu TT, Xie JQ, Ren F (2014) Short glass fiber reinforced radiation crosslinked shape memory SBS/LLDPE blends. *J Appl Polym Sci* 131:40691. <https://doi.org/10.1002/App.40691>